High-resolution Ar L-shell Auger spectroscopy in 80-MeV Ar^{5+} + He collisions

P. Focke,* T. Schneider, D. Schneider, G. Schiwietz, I. Kádár,† and N. Stolterfoht
Hahn-Meitner-Institut Berlin GmbH, Glienickerstrasse 100, D-1000 Berlin 39, Federal Republic of Germany

J. E. Hansen
Zeeman Laboratorium, Universiteit van Amsterdam, Plantage Muidergracht 4, NL-1018 TV Amsterdam, The Netherlands
(Received 1 June 1989)

Auger-electron spectra produced in the collision of 80-MeV Ar^{5+} + He were measured with high resolution. The spectra are dominated by the Auger decay of the Ar^{6+} projectile in a configuration with a hole in the $2p$ shell. All of the observed transitions can be identified by means of multiconfiguration calculations for transition energies. The line intensities are compared with transition rate calculations using the intermediate-coupling scheme. The observation of an Auger transition, which is forbidden in the single-configuration picture, is interpreted as being due to electron-correlation effects.

I. INTRODUCTION

In the study of highly charged ions, the spectroscopy of Auger electrons produced in energetic ion-atom collisions is a valuable method for obtaining detailed information about fundamental atomic processes. The analysis of the Auger spectra allows the study of the atomic structure as well as of the excitation mechanism for the inner-shell vacancy states involved.[1] The atomic structure information may be used as a test of fundamental theories in many-body problems.

A particularly useful tool in this study is the projectile Auger spectroscopy.[2] It has the advantage that incident highly charged states may be produced by stripping the projectile prior to the experiment. In addition, the Doppler shift of the emitted electrons results in a stretching effect that enhances the resolution of spectral structures.[1] On the other hand, serious problems are involved due to kinematic line-broadening effects. These undesirable effects can, to a large extent, be avoided by measuring the Auger electrons under an observation angle of 0°. The method of 0° Auger spectroscopy, extensively applied in recent years, has proven to yield excellent spectral resolution.[3,4]

Another serious problem involved in Auger spectroscopy is the copious number of states normally produced in violent ion-atom collisions. This may result in a considerable blending of the observed Auger lines, which complicates the identification of the transitions involved. Fortunately, the number of states can be significantly reduced by using light target atoms, such as hydrogen or helium. Low-Z target particles, when ionizing the inner shell, do not substantially disturb the outer shells. This inner-shell ionization may be considered as an example for the method[1,4] where a specific electron is removed without affecting the configuration of the other electrons much. Hence, the number of initial states which is produced is limited.[3,4]

A challenging application of this "ion surgery" method is the analysis of L-shell Auger-electron spectra, which are characterized by their complexity.[5,6] The spin-orbit interaction in the initial states, as well as in the final states, considerably increases the number of possible Auger transitions. A typical L-shell Auger spectrum contains numerous lines and peak structures are generally associated with groups of overlapping lines. Typical examples of the serious difficulties encountered in the analysis of L-shell Auger spectra in the past are the studies of the transitions from the Mg-like and Na-like configurations, which have been performed on diverse ionic projectiles.[7,8] In these circumstances inner-shell ionization in conjunction with zero-degree Auger spectroscopy is particularly well suited. First high-resolution measurements made by Itoh *et al.*[3] in Ar^{5+} + He collisions showed that, indeed, the Auger spectra are remarkably simple. They consist of well-separated peak groups associated primarily with transitions from the Mg-like initial configurations.

An interesting feature in those spectra is the lowest energy group which has been identified as being due to a three-electron transition.[9] Using a completely different experimental method, Malutzki *et al.*[10] studied the Auger spectra of atomic Al following $2p$ photoionization. They observed the transitions from the Mg-like initial configuration $1s^2 2s^2 2p^5 3s^2 3p$ (hereafter, the passive part $1s^2 2s^2$ is not repeated any more in the configuration label) and classified practically all observed Auger lines. In particular, they identified the equivalent of the three-electron transition, discussed above for Ar^{6+}, thus providing additional evidence for such a process.

In this work we applied the method of 0° Auger spectroscopy to study the Ar L-shell Auger spectra in the collision system Ar^{5+} + He. We present a detailed analysis of the Auger-electron spectra. In particular, we have analyzed the Auger lines attributed to the Mg-like configuration $2p^5 3s^2 3p$ of Ar^{6+}. The measured Auger-electron energies and intensities are used to verify results obtained within the framework of atomic structure theories.

II. EXPERIMENTAL METHOD AND DATA ANALYSIS

The experiments were performed with the heavy-ion accelerator facility VICKSI at the Hahn-Meitner-Institut in Berlin. The apparatus used in the measurements has been described elsewhere.[3,11] A beam of Ar^{5+} with an energy of 80 MeV was passed through a 10-cm long target cell containing He gas. The gas pressure was a few 10^{-2} Torr. Care was taken to retain single-collision conditions.[11]

The electrons ejected from the projectile were analyzed with an electrostatic electron spectrometer. The spectrometer consists of two parallel-plate electrostatic analyzers combined in tandem.[3] One spectrometer with relatively large slits has the purpose of deflecting the electrons out of the beam direction. The electrons are then directed into the second spectrometer which is used for the energy analysis. For high-resolution measurements a decelerating electric field was applied to the electrons prior to entering the high-resolution analyzing spectrometer. During the measurement the analyzing spectrometer was operated by applying a varying decelerating voltage to the electrons prior to entering the spectrometer and a fixed voltage was applied across the plates of this spectrometer. In this way it was ensured that all of the structures in the electron spectra were measured with equal energy resolution.

In Fig. 1 we show an example of such a transformed spectrum for 79.4-MeV Ar^{5+} incident on He. The electron spectra measured in the laboratory reference frame were transformed to the projectile reference frame[3] taking into account relativistic corrections. This spectrum displays the structures of interest for the present discussion. It can be seen in Fig. 1 that, as expected, a relatively simple spectrum is obtained by using the light target atom He. In the Auger-electron energy range studied the He target mainly removes one electron from the L shell leaving the other shells intact. The ground-state configuration of $Ar^{5}+$ is $2p^{6}3s^{2}3p$, so that the most prominent peak groups in Fig. 1 correspond to the decay of the $2p^{5}3s^{2}3p$ configuration. The states associated with this configuration are shown in Table I and Fig. 2.

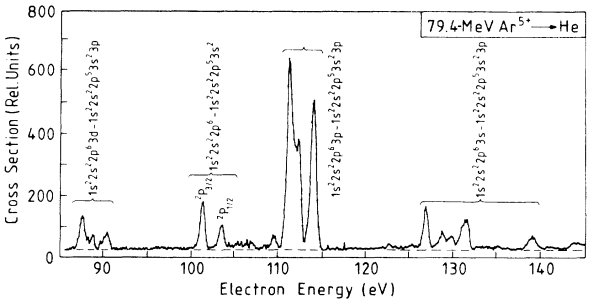

FIG. 1. L-shell Auger spectrum of Ar produced in the collision of 79.4-MeV Ar^{5+} on He. The observation angle is 0°. The electron energy refers to the projectile frame. Three groups of lines are assigned to transitions from the initial configuration $2p^{5}3s^{2}3p$ of Ar^{6+} to the final ones $2p^{6}3d$, $2p^{6}3p$, and $2p^{6}3s$, respectively. Two lines result from the decay of the $2p^{5}3s^{2}$ ($^{2}P_{3/2}$), ($^{2}P_{1/2}$) levels of Ar^{7+} to $2p^{6}$.

Figure 1 shows four groups of lines, some of which have been interpreted in the previous paper by Itoh *et al.*[3] The groups centered at 112 and 130 eV were identified as belonging to the transitions from the configuration $2p^{5}3s^{2}3p$ of Ar^{6+} to the final configurations $2p^{6}3p$ and $2p^{6}3s$, respectively. The structure in these groups originate from the angular momentum coupling of the two unfilled shells $2p$ and $3p$ in the initial configuration. The interpretation of the group at 89 eV was unclear at the time of the initial interpretation. Later it was identified[1,9] as being due to transitions from the same initial configuration $2p^{5}3s^{2}3p$ of Ar^{6+} to the configuration $2p^{6}3d$, with the same relative energy pattern as shown by the other two groups at 112 and 130 eV. Moreover, the isolated Auger line at 138.6 eV results from the same type of transition assigned to the group at 130 eV, so that it is interpreted as being a member of this group. In the other two groups this line is not visible within the statistical fluctuations of the background.

TABLE I. Square of the expansion coefficients of intermediate coupling states specified by the total angular momentum and the largest eigenvector component present in the $2p^{5}3s^{2}3p$ configuration. The basis is composed of LS coupled states formed from the indicated Mg-like configurations of Ar^{6+}. For the $2p^{5}3s^{2}3p$ configuration contributions to individual terms are given. Energy values are given relative to the $2p^{6}3s\ ^{2}S_{1/2}$ state of Ar^{7+}.

State	J	Energy (eV)	$3s^{2}3p$ ^{3}S	^{3}D	^{3}P	^{1}S	^{1}D	^{1}P	$3s3p3d$ all	$3p3d^{2}$ all
$^{3}S_1$	1	126.70	0.90	0.00	0.05				0.021	0.002
$^{3}D_3$	3	128.35		0.95					0.022	0.002
$^{3}D_2$	2	128.48		0.67	0.06		0.22		0.023	0.002
$^{3}D_1$	1	129.13	0.004	0.47	0.18			0.29	0.022	0.002
$^{3}P_2$	2	129.57		0.008	0.61		0.33		0.024	0.002
$^{1}P_1$	1	130.69	0.000	0.47	0.12			0.35	0.022	0.002
$^{3}P_0$	0	130.83			0.94	0.013			0.025	0.002
$^{1}D_2$	2	131.24		0.29	0.25		0.42		0.023	0.002
$^{3}P_1$	1	131.37	0.05	0.005	0.60			0.29	0.023	0.002
$^{1}S_0$	0	138.34			0.013	0.92			0.031	0.002

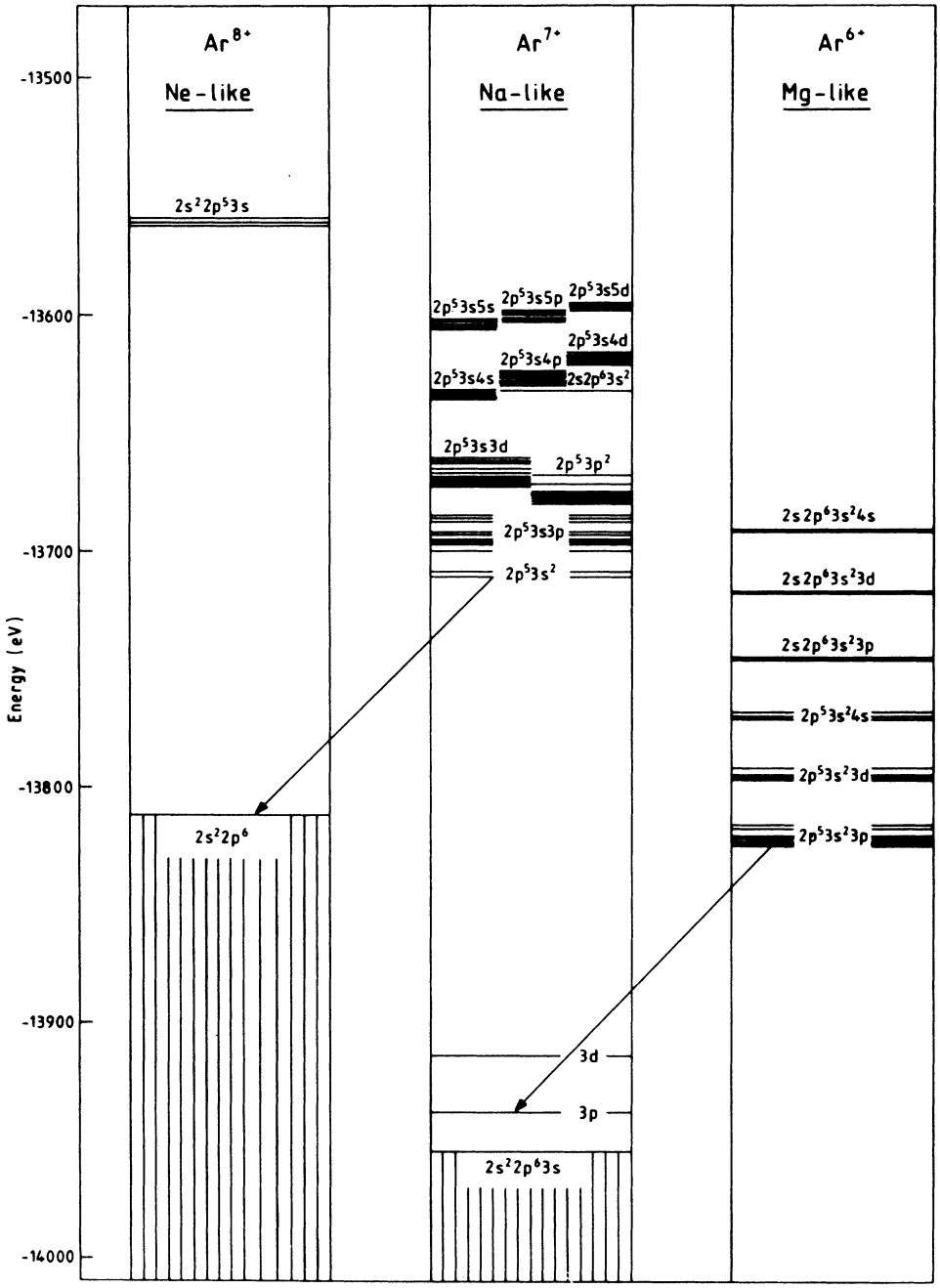

FIG. 2. *L*-shell Auger transition diagram for Ar ions. The arrows indicate the observed transitions in Fig. 1. The diagram is based on calculations using the Dirac-Fock code due to Grant and co-workers (Ref. 12). From Ref. 1.

The two single peaks located at 101.5 and 103.7 eV were ascribed[3] to the transition from the Na-like configuration $2p^5 3s^2$ of Ar^{7+} to the final configuration $2p^6$ of Ar^{8+}. The two lines result from the spin-orbit splitting of the initial state into the levels $^2P_{3/2}$ and $^2P_{1/2}$. From the presence of the Na-like Ar^{7+} ion it is seen that the additional ionization of the single $3p$ electron in the outer M shell is possible. Under the assumption that the Auger decay of the configurations $2p^5 3s^2$ and $2p^5 3s^2 3p$ produce only the lines seen in Fig. 1 with an isotropic distribution and that the fluorescence yield is negligible, the intensities of the lines are a direct measure of the ratio between the cross sections for the emission of a $2p$ electron and for the simultaneous emission of a $2p$ and a $3p$ electron. Hence, this intensity ratio is a measure for the ratio of the cross section for producing Na-like Ar to the cross

section of producing Mg-like Ar. The measurements show that the intensity of the Na-like doublet at 102.5 eV is about 10% of the intensity arising from the decay of the Mg-like configuration $2p^5 3s^2 3p$.

In order to obtain detailed information about the line structures we performed a decomposition of the three groups of lines from the Mg-like configuration into their individual components. Before fitting we subtracted a smooth continuous background which results from other electron-emission processes such as direct ionization. The fitting procedure was carried out using the same line shape for all peaks. This line shape was obtained from the decay of the Na-like configuration in Ar^{7+} which produces the isolated lines at 101.5 eV, as mentioned previously. The natural width Γ of the Auger lines, was calculated to be less than 0.001 eV for all the lines in the spectrum. Hence, in our case the Auger line shape is basically determined by the spectrometer response function. This justifies the assumption of a fixed line shape.

The intensities and energy positions of the lines were determined by applying a fitting procedure. The results of the line fit are plotted in Fig. 3. In Table II we show the measured energies and the relative intensities. Only four of the expected ten lines could be resolved. Three pairs of lines, which were theoretically predicted to lie within about 0.1 eV of each other, could not be separated in our measured spectra with the present experimental resolution. The origin of the theoretical results in Table II is explained in the next section.

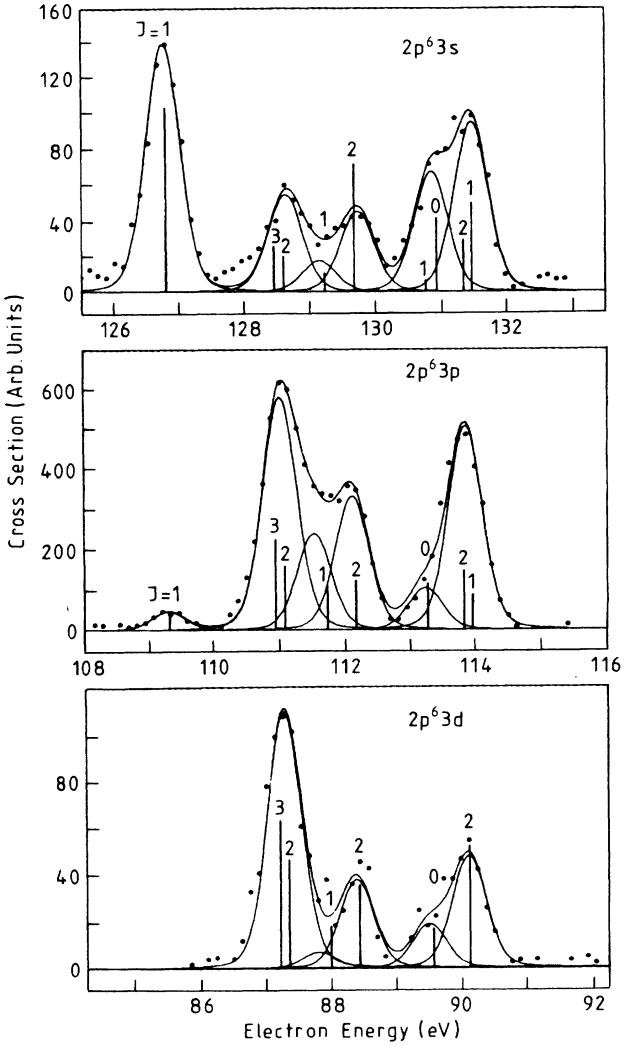

FIG. 3. Line structure of Auger transition spectra from Ar^{6+}. The initial configuration is $2p^5 3s^2 3p$ and the final configuration is indicated in the figure. The vertical lines refer to theoretical transition energies and intensities as given in Table II. The individual lines are specified by the total angular momentum in the initial state of the transition.

III. THEORETICAL METHOD

In order to verify the above-mentioned line assignments and spectral structure, single-configuration Dirac-Fock (DF) calculations have been carried out using the program due to Grant and co-workers.[12] The results of the calculations are summarized graphically in Fig. 2, where the experimentally observed groups of transitions are indicated with arrows.[1] For the Mg-like transitions the term and fine-structure splitting in the initial configuration are of the same magnitude so that the intermediate-coupling scheme is appropriate for the present description.

The individual decay rates for the transitions in the Ar L-shell Auger spectrum were calculated using the configuration-interaction Hartree-Fock (CIHF) program developed by Cowan.[13] The calculations were similar to those carried out by Malutzki *et al.*[10] for the analogous case of Al with a hole in the $2p$ shell. The only difference is that nonrelativistic HF calculations were used to construct the basis set for Al^+ while we have used the approximate relativistic HF method (HFR), due to Cowan and Griffin,[14] to construct basis states for Ar^{6+}, since it was felt that relativistic effects might be important for the latter ion due to the higher degree of ionization. However, very small differences were found between HF and HFR values.

For the description of the initial state i all states arising from the configurations $2p^5 3s^2(3p+4p+5p)$, $2p^5 3s 3p 3d$, $2p^5 3p 3d^2$, and $2p^5 3p^3$ have been included. The last three configurations belong to the same complex[15] of configurations interacting most strongly with $2p^5 3s^2 3p$. The $4p$ and $5p$ configurations are included because of well-known difficulties in the description of the S terms in $2p^5 3p$ using a single-configuration approach.[16] In order to obtain a good description of the S terms it is, in principle, necessary to include the whole np-ϵp series in a CI expansion. To compensate for the fact that a limited number of p configurations are included, we have scaled down the HF values for the exchange integrals within configurations by 10%. The final state f has the

TABLE II. Energies and intensities of L-shell Auger lines of Ar^{6+}. The initial states are specified as in Table I. The theoretical values were calculated with the configuration-interaction Hartree-Fock program of Cowan (Ref. 13). For the theoretical intensities a $2J+1$ population of the initial states was assumed. The absolute and relative values of the experimental energies are uncertain by 0.5 and 0.2 eV, respectively. The theoretical and experimental intensities are normalized to the same total value of 100.

Auger decay			Energy (eV)		Relative intensity	
Initial state		Final state	Theory	Expt.	Theory	Expt.
$2p^5 3s^2 3p$	$^3S_1$	$2p^6 3s^2 S$	126.70	126.7	6.37	5.5(4)
	$^3D_3$		128.35	128.4	1.61	2.1(3)
	$^3D_2$		128.48		1.30	
	$^3D_1$		129.13	128.9	0.58	0.67(22)
	$^3P_2$		129.57	129.5	3.64	1.7(2)
	$^1P_1$		130.69	130.6	0.42	2.7(6)
	$^3P_0$		130.83		2.59	
	$^1D_2$		131.24	131.2	174	3.8(5)
	$^3P_1$		131.37		3.06	
	$^1S_0$		138.34	138.6	2.66	0.42(8)
$2p^5 3s^2 3p$	$^3S_1$	$2p^6 3p^2 P$	109.11	109.2	1.97	1.9(3)
	$^3D_3$		110.76	110.9	13.9	23.7(12)
	$^3D_2$		110.89		9.76	
	$^3D_1$		111.54	111.4	6.66	97.(19)
	$^3P_2$		111.98	112.0	5.99	13.5(24)
	$^1P_1$		113.10	113.1	6.90	4.2(8)
	$^3P_0$		113.24		0.17	
	$^1D_2$		113.65	113.7	9.01	20.6(13)
	$^3P_1$		113.78		5.20	
	$^1S_0$		120.75		0.12	
$2p^5 3s^2 3p$	$^3S_1$	$2p^6 3d^2 D$	85.45		0.007	
	$^3D_3$		87.10	87.3	3.84	4.7(6)
	$^3D_2$		87.23		2.83	
	$^3D_1$		87.88	87.8	1.08	0.29(9)
	$^3P_2$		88.32	88.4	4.27	1.6(3)
	$^1P_1$		89.44	89.5	1.05	0.78(18)
	$^3P_0$		89.58		0.01	
	$^1D_2$		89.99	90.1	3.17	2.0(2)
	$^3P_1$		90.12		0.07	
	$^1S_0$		97.09		0.004	
			Sum of all intensities:		100	100

form $2p^6 3l\epsilon l'$, where l stands for s, p, or d and l' stands for p, d, f, or g. The Auger transition rates were calculated using the perturbation theory expression (in a.u.):

$$\dot{P}_{if} = 2\pi \left| \left\langle f \left| \sum_{k>l} r_{k,l}^{-1} \right| i \right\rangle \right|^2 .$$

No interchannel configuration interaction was allowed in the final state. This approximation is usually not considered to be very serious for high energies of the ejected electron.

The result of the CIHF energy calculation is shown in Table I. The energies are given relative to the $2p^6 3s\ ^2S_{1/2}$ state but only the relative energies within the configuration are *ab initio* values. The absolute energies have been calibrated to fit the experimental $^3S_1$ peak. A similar table has been presented earlier[1] but the present calculation is considered to be slightly more accurate. The level splittings arising from the spin-orbit coupling in the final configurations $2p^6 3p$ and $2p^6 3d$ are not relevant under the present experimental conditions since these splittings are smaller than 0.3 eV, which is less than the spectrometer resolution of 0.6 eV. This means that the *relative* energies in Table I also will describe the decay to the latter configurations. The absolute theoretical energies for these decays given in Table II are obtained by subtracting the known $3p$ and $3d$ excitation energies[17] in Ar^{7+} from the energies in Table I.

TABLE III. Transition rates for the Mg-like ion Ar^{5+}. The initial states are identified by the *LS* term as specified in Table I. The transition probabilities are summed over the fine-structure levels of the final state.

Initial state		Final state Transition probability (sec^{-1})		
		$2p^6 3s(^2S)$	$2p^6 3p(^2P)$	$2p^6 3d(^2D)$
$2p^5 3s^2 3p$	$^3S_1$	1.21×10^{13}	3.74×10^{12}	1.26×10^{10}
	$^3D_3$	3.10×10^{11}	2.69×10^{12}	7.42×10^{11}
	$^3D_2$	2.52×10^{11}	1.90×10^{12}	5.50×10^{11}
	$^3D_1$	2.01×10^{11}	2.29×10^{12}	3.73×10^{11}
	$^3P_2$	5.87×10^{10}	9.66×10^{10}	6.89×10^{10}
	$^1P_1$	1.50×10^{11}	2.45×10^{12}	3.73×10^{11}
	$^3P_0$	6.14×10^{12}	4.13×10^{11}	2.51×10^{10}
	$^1D_2$	1.57×10^{11}	8.15×10^{11}	2.87×10^{11}
	$^3P_1$	7.26×10^{11}	1.23×10^{12}	1.70×10^{10}
	$^1S_0$	4.23×10^{14}	1.89×10^{13}	6.49×10^{11}

An inspection of the mixing coefficients in Table I shows the strong coupling among the terms in the $2p^5 3s^2 3p$ configuration of Ar^{6+} and, hence, the importance of the intermediate-coupling scheme for this configuration. To help distinguish between levels with the same value of J we use the largest eigenvector component from Table I. This leads to unambiguous labels for all levels, except two $J=1$ levels, which both have $^3D_1$ as the largest eigenvector component, while no level exists with $^1P_1$ as the largest component. Consequently we have called the level with higher $^1P_1$ component $^1P_1$.

The summed contributions to the eigenvectors from the $2p^5 3s 3p 3d$ and $2p^5 3p 3d^2$ configurations shown in Table I are very small and could give the impression that the Auger decay to $2p^6 3d$, that can take place because of these admixtures, must be very small. However, the transition rate depends also on the radial matrix element. Thus, despite the very small eigenvector components involving a $3d$ electron, the decay rates to $2p^6 3d$ are substantial as shown in Table III and discussed further below.

IV. DISCUSSION OF THE RESULTS

The comparison of the theoretical and experimental transition energies shows agreement to within 0.3 eV. The line at 138.6 eV, that decays from the initial state ($^1S_0$) is separated by 7.4 eV from the next nearest line (assigned to $^3P_1$ and $^1D_2$). This isolated line ($^1S_0$) was only observed for the transition $2p^6 3s$-$2p^5 3s^2 3p$. The initial ^1S state for this transition is located above the other levels due to the large effect of exchange for this term.[18,19]

The intensity distribution of the lines in the groups is determined by the relevant transition rates $\dot{P}_{if}$ for Auger decay, which are shown in Table III as they resulted from the CIHF calculation.[13] As seen from Table III, the general trend of the transition probabilities is to favor the decay to the final configuration $2p^6 3p$. This is also clearly seen in Fig. 1 and Table II. But there are some remarkable exceptions. The lowest-lying ($^3S_1$) state is found to decay preferentially to the final configuration $2p^6 3s$. The same behavior is observed for the highest-lying state ($^1S_0$). Obviously there is no selection rule which forbids transitions from these states to final configurations other than $2p^6 3s$. From Table I it is seen that these two states have the common feature of being described with high purity by an S term. The same behavior was observed[10] in Al and it was shown that the reason for the large decay rates to $3s$ is that these two terms can decay with an outgoing s wave to $3s$. The s wave has the largest overlap with the bound electron but can couple to an S term only with the $3s$ final state.

Since the initial populations of the individual $2p^5 3s^2 3p$ levels are unknown, the theoretical transition probabilities can only be used reliably to compare branching ratios from a particular final state to the three final states. For those features which consist of two unresolved lines, a comparison is not possible without an assumption about the initial population. Consequently, we have chosen to calculate theoretical relative intensities (Table II) under the assumption that *all* initial levels are uniformly populated with a statistical weight of $2J+1$. Thus, the sum of the transition probabilities to the three final states is proportional to $2J+1$ and the total sum has been normalized to 100, as has also been done with the experimental values. Nevertheless, it should be kept in mind that only the branching ratios for the resolved lines can unambiguously be compared with experiment.

Table II shows that the theoretical intensities follow the general trend of the experiment but some notable differences are present. For instance, a significant discrepancy is seen for the resolved lines attributed to the three transitions from the initial state $^3P_2$. Here the intensity calculated for the transitions to $3s$ and $3d$ are too large while the intensity to $3p$ is too small. The ^3P term cannot decay to the $3s$ in the absence of spin-orbit interaction and it can be seen from Table III that the transition probability to $3s$ for the ^3P term is the lowest of all. It is therefore not so surprising that the calculated values for this term are less accurate than for the others. Nevertheless the discrepancy indicates that the mixing between terms is less than perfect. The calculated transition probabilities for the other ^3P levels are also fairly weak but since the associated lines are unresolved it is difficult to compare these values with experiment. The rather large value calculated for the decay of $^3P_0$ to $3s$ is due to a small admixture of $^1S_0$ for this level.

Also, for the line associated with the initial level $^1S_0$ there is a discrepancy for the decay to $3s$. However, since, in this case, the calculated branching ratio shows good agreement with the observation that only decay to $3s$ is observed, the disagreement for this line intensity means that the $^1S_0$ level is populated less than expected on statistical grounds. The same was observed in Al although the excitation mechanism in that case was completely different.[10] For the other levels the deviations from statistical population do not seem to be very large. However, it must be kept in mind that most other levels

have larger J values and thus a larger population in absolute terms, so that absolute errors of the same size as for $^1S_0$ in relative terms are smaller. It is thus possible that the large deviation from statistical population for $^1S_0$ is magnified by deviations in the populations of the other levels which are less visible in the data.

The results for the calculated and observed branching to the three final terms summed over all initial states in Ar^{6+} are summarized in Table IV along with previous data for Al^+. It should be kept in mind that the theoretical data are obtained under the assumption that the initial levels are populated proportionally to $2J+1$. We note in particular the large change in the $3s$-$3p$ branching when going from Al^+ to Ar^{6+} with $3s$ becoming weaker with increasing degree of ionization. All interaction integrals with the contunua increase with increasing ionization but many of the integrals are negative in Al and thus smaller in absolute value in Ar. The result is that the interaction with the $3s\epsilon s$ and $3p\epsilon p$ continua is larger in Ar than in Al while the interaction with $3s\epsilon d$ is smaller. Since only the levels with S character can reach the $3s\epsilon s$ continuum, the levels with $J>1$, which carry a large part of the statistical weight, decay preferentially to $3p$ with increasing ionization.

The peak group at 89 eV is particularly interesting. The good agreement between theoretical and experimental transition energies and the same energy pattern for the three groups of Auger lines identified as having their origin in Ar^{6+} excludes any doubts about the interpretation[9] of the peak group at 89 eV as being due to the transition $2p^63d$-$2p^53s^23p$. The comparison of the initial and final configurations indicates that three electrons participate in the Auger decay.[9,10] This three-electron process is not allowed, assuming unperturbed initial and final configurations. In the CI description of the initial states from which the transition probabilities shown in Table III were determined, electron-correlation effects were included through the interaction with the configurations within the complex.[15] This bound-state configuration interaction accounts for the fact that transitions to the configuration $2p^63d$ is possible in our calculation.

A comparison of the theoretical and experimental total intensities of the three groups indicates that this description is still incomplete. Table IV shows that the predicted value for the decay to $2p^63d$ in Ar^{6+} is significantly higher than the experimental result, whereas in Al^+ the corresponding intensity is smaller than observed. The agreement between calculated and experimental intensities is somewhat better in Al^+ than in Ar^{6+}. It is difficult to see why basically the same calculation should give a significant difference for this intensity for two spectra so close together in the isoelectronic sequence. Why the calculation as such should be significantly worse in Ar^{6+} than in Al^+ it is not clear. In particular, there is more cancellation in the forming of the radial integrals for Al than for Ar.

In an effort to understand the reason for the deviations, we have carried out calculations with a larger expansion, including $2p^53s^26p$ and $2p^53p^24p+2p^54p^23p$ using both HF and HFR basis states. This calculation led to a slight improvement in the branching for $^3P_2$ but did not change the branching between the three final configurations in Table IV.

To explain the discrepancies between experiment and theory, one may consider anisotropic angular distributions of the ejected electrons due to alignment effects. It is recalled that, in this work, we determined differential cross sections for electron emission at zero degree only and we assumed isotropic electron emission to obtain integrated cross sections. There are good arguments for the isotropic electron emission. In previous studies negligible alignment effects were found in the case of $2p$ ionization of (neutral) Ar by light particle impact (protons and helium).[20] Furthermore, if alignment effects are present, they should influence not only the data for the decay to the final state $2p^63d$ but also those attributed to the decay to $2p^63s$ and $2p^63p$. In the latter cases, however, quite a good agreement was found between theoretical and experimental line intensities. However, it is noted that, unlike in neutral Ar, in Ar^{5+} there is an electron outside closed shells which may explain that the ^1S state apparently is not statistically populated.

Alternatively, one may consider interchannel configuration interaction which is not included into the final state, as mentioned earlier. This effect is usually not large at high electron energies but has been observed, for example, in the K-LL Auger spectrum[21,22] of Ne. It is difficult to see why the effect should be substantially different in Al^+ and Ar^{6+}. It should be noted, however, that the contribution of the interchannel configuration interaction adds coherently. One may speculate that the matrix element, responsible for the interchannel configuration interaction changes sign and, thus, the effect adds constructively for Al^+ and destructively for Ar^{5+}. This may be visualized in a simple picture which for Al^+ has the outgoing Auger electron hitting the $3p$ electron and transferring it to the $3d$ orbital whereas in Ar^{5+} a $3d$ electron, which is present because of initial-

TABLE IV. Intensities of Auger line groups attributed to different final states. The data for Ar^{6+} are obtained summing the intensities for the associated lines in Table II. The data for Al^+ are from Ref. 10. The theoretical and experimental intensities are normalized to the same total value of 100.

Auger transition between initial configurations	final configurations	Relative intensity Al^+ Theory	Al^+ Expt.	Ar^{6+} Theory	Ar^{6+} Expt.
$2p^53s^23p$	$2p^63s$	46	46	24	17(1)
	$2p^63p$	43	39	60	73(2)
	$2p^63d$	12	16	16	9(1)

state configuration interaction, is transferred down to the $2p$ orbital by the Auger electron. It is felt that the inclusion of interchannel interaction between the continuum states would be useful in pinning down the reason for the discrepancy. It would also be useful to try an alternative treatment of the Auger decay, for example, by using many-body perturbation theory in higher order as developed by Kelly,[21] or using the scattering approach of Åberg.[22]

V. CONCLUSION

In conclusion, we have measured Auger-electron spectra of multiply charged Ar ions with high resolution. We observed transitions from the configurations $2p^5 3s^2 3p$ of Ar^{6+} and $2p^5 3s^2$ of Ar^{7+}. All of the observed transitions could be identified with the help of DF calculations[12] and CIHF calculations[13] which show that the theoretical data may provide a valuable assistance in the task of line assignment. The decay of Ar^{6+} presented a rich spectrum which could be assigned to the initial-state level splitting. In order to account correctly for the observed structure, it was essential to treat the level structure in intermediate coupling. It was found that the $2p^5 3s^2 3p\ ^1S_0$ level has a lower population after the collision than expected on statistical grounds. In addition, an Auger decay was observed, which is forbidden in the single-configuration picture, thus providing evidence for the importance of including electron-correlation effects in the description of atomic states. A better understanding of the Auger transition mechanism is expected if higher-order effects are taken into account.

ACKNOWLEDGMENTS

We are much indebted to Vic Montemayor for helpful comments on the present work. We thank A. Itoh for his assistance in the pioneering stage of the present study. The CIHF calculations were performed on the CYBER 205 computer in Amsterdam under Grant No. SC-20 from the foundation SURF (The Cooperative Body for the Advancement of Computer Services in High Education and Scientific Research).

---

*Permanent address: Centro Atomico Bariloche, 8400 Bariloche R.N., Argentina.

†Permanent address: Institute of Nuclear Research, Bem-tér 18c, H-4001 Debrecen P.F. 51, Hungary.

[1]N. Stolterfoht, Phys. Rep. **146**, 315 (1987).

[2]I. A. Sellin, in *Beam Foil Spectroscopy*, Vol. I of *Topics in Current Physics*, edited by S. Bashkin (Springer, Heidelberg, 1976), p. 265.

[3]A. Itoh, T. Schneider, G. Schiwietz, Z. Roller, H. Platten, G. Nolte, D. Schneider, and N. Stolterfoht, J. Phys. B **16**, 3965 (1983).

[4]N. Stolterfoht, P. D. Miller, H. F. Krause, Y. Yamazaki, J. K. Swenson, R. Bruch, P. F. Dittner, P. L. Pepmiller, and S. Datz, Nucl. Instrum. Methods **B24-25**, 168 (1987).

[5]D. J. Voltz and M. E. Rudd, Phys. Rev. A **2**, 1395 (1970).

[6]N. Stolterfoht, D. Schneider, and H. Gabler, Phys. Lett. **47A**, 271 (1974).

[7]P. Dahl, M. Rødbro, G. Hermann, B. Fastrup, and M. E. Rudd, J. Phys. B **9**, 1581 (1976).

[8]T. Matsuo, H. Shibata, J. Urakawa, M. Sekiya, A. Yagishita, T. Kambara, M. Kase, and Y. Awaya, J. Phys. B **21**, 1791 (1988).

[9]N. Stolterfoht, T. Schneider, D. Schneider, and A. Itoh, in *Proceedings of the XIV International Conference on the Physics of Electronic and Atomic Collisions, Abstracts*, edited by M. J. Coggiola, D. L. Huestis, and R. P. Saxon (University Press, Stanford, 1985), p. 467.

[10]R. Malutzki, A. Wachter, V. Schmidt, and J. E. Hansen, J. Phys. B **20**, 5411 (1987).

[11]A. Itoh, D. Schneider, J. T. M. Zouros, G. Nolte, G. Schiwietz, W. Zeitz, and N. Stolterfoht, Phys. Rev. A **31**, 684 (1985).

[12]I. P. Grant, I. McKenzie, P. H. Norrington, D. F. Meyers, and N. C. Pyper, Comp. Phys. Commun. **21**, 207 (1980).

[13]R. D. Cowan, *The Theory of Atomic Structure and Spectra* (University of California Press, Berkeley, 1981), Chaps. 7–14.

[14]R. D. Cowan and D. C. Griffin, J. Opt. Soc. Am. **66**, 1010 (1976).

[15]D. Layzer, Ann. Phys. (N.Y.) **8**, 271 (1959).

[16]J. E. Hansen, J. Phys. B **6**, 1387 (1973).

[17]B. Edlén, Phys. Scr. **17**, 565 (1978).

[18]E. U. Condon and G. H. Shortley, *The Theory of Atomic Spectra* (University Press, Cambridge, 1964).

[19]J. E. Hansen, J. Phys. B **6**, 1751 (1973).

[20]N. Stolterfoht, D. Schneider, and P. Ziem, Phys. Rev. A **10**, 81 (1974).

[21]H. P. Kelly, Phys. Rev. A **11**, 556 (1975).

[22]T. Åberg, Phys. Scr. **21**, 495 (1980).